Langmuir

ARTICLE

pubs.acs.org/Langmuir

Honeycomb-Patterned Film Segregated with Phenylboronic Acid for Glucose Sensing

Peng-Cheng Chen, Ling-Shu Wan,* Bei-Bei Ke, and Zhi-Kang Xu

MOE Key Laboratory of Macromolecular Synthesis and Functionalization, Department of Polymer Science and Engineering, Zhejiang University, Hangzhou 310027, China

Supporting Information

ABSTRACT: Phenylboronic acid (PBA)-functionalized materials have attracted considerable attention because of their potential applications in many fields. In this paper, we report a PBA-segregated honeycomb-patterned porous film (HPPF) for glucose sensing. Polystyrene-*block*-poly(acrylic acid-*co*-acrylamidophenylboronic acid) with different contents of PBA pendants was synthesized via atom transfer radical polymerization (ATRP) followed by a coupling reaction. PBA-functionalized HPPFs were then fabricated by the breath figure method. Results indicate that the composition of the copolymers and the relative humidity play key roles in pore size and regularity of the films. Using Alizarin Red S (ARS) that does not emit fluorescence itself as a fluorescent probe, it is confirmed that PBA pendants are mainly distributed at the pore wall, instead of at the outer surface of HPPFs. This distribution is caused by the segregation of hydrophilic PBA-blocks toward the condensed water droplets, which act as templates for the pore formation. Quartz crystal microbalance results demonstrate that the PBA-functionalized HPPFs show high sensitivity in glucose sensing, which is owing to the segregation of PBA pendants at the pore wall as well as the large specific surface area of the porous films.

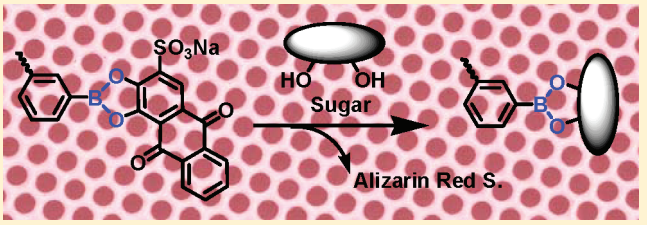

INTRODUCTION

Functional materials with ordered pores have received increasing interest because of their potential applications as photonic crystals,[1] sensors,[2] membranes,[3] catalyst supports,[4] microreactors,[5] and so on. Lithography techniques have often been used for preparing ordered porous materials,[6] which are time-consuming and require special equipment. As an alternative method, the recently developed breath figure (BF) method exhibits fascinating advantages of convenient operation and cost-efficiency.[7−10] In a BF process, the foggy array of water droplets induced by solvent evaporative cooling acts as sacrificial templates for spherical pores and leaves a honeycomb-patterned porous film (HPPF) after further evaporation. A variety of polymers, including linear homopolymers, star polymers, hyperbranched polymers, comblike copolymers, and rod−coil/coil−coil block copolymers, have been employed to fabricate such films with pore diameters ranging from 100 nm to 20 μm.[7−14]

Up to now, HPPFs have been applied to various fields including superhydrophobic materials, catalyst supports, surface enhanced Raman scattering (SERS) substrates, cell culture substrates, sensors, and protein arrays.[15−21] Various functionalization approaches have been developed to satisfy the requirements of these applications. Among the approaches, utilization of the segregation of polar end groups,[22,23] hydrophilic blocks,[24−26] water-soluble additives,[27,28] or particles[29−32] during the BF process is very promising because this method is simple and mostly site-selective. The segregation generally occurs at the interface of the condensed water droplets and the organic solution, leading to in situ functionalization of the pore wall. Nevertheless, how to convincingly prove the segregation of end groups or blocks remains a challenge. Particles embedded or attached at the pore wall could be directly observed by TEM or SEM.[29−32] For some systems AFM is a powerful tool to reveal the phase separation.[33] Bacteria were also used to distinguish the hydrophilic and hydrophobic areas of HPPFs.[10] As far as we know, ToF-SIMS imaging (time-of-flight secondary-ion mass spectrometry) is the only successful chemical characterization of the segregation of end groups or blocks in HPPFs;[22] other techniques such as XPS imaging and FTIR microscopy do not work well because of their low resolution compared with the pore size of HPPFs. In previous works by us and other researchers, 2D and 3D fluorescence images were obtained to visualize the segregation after the reaction of the enriched groups with fluoresceins.[22−25] It should be noted that this method cannot completely avoid fluorescence background induced by fluorescein adsorption. Therefore, it is interesting to find a system for convincing elucidation of surface segregation of hydrophilic blocks and for construction of functional materials based on the segregation.

Phenylboronic acid (PBA) is a well-known molecular receptor that can bind with compounds containing *cis*-diol moieties.[34] The binding is of high affinity through reversible formation of boronate, which is the principle behind its applications in the fields of sensing carbohydrates, nucleotide, coenzymes,

Received: May 21, 2011
Revised: September 3, 2011
Published: September 07, 2011

ACS Publications © 2011 American Chemical Society

dx.doi.org/10.1021/la201911f | *Langmuir* 2011, 27, 12597–12605

Scheme 1. Synthesis of PS-*b*-P(AA-*co*-AAPBA)

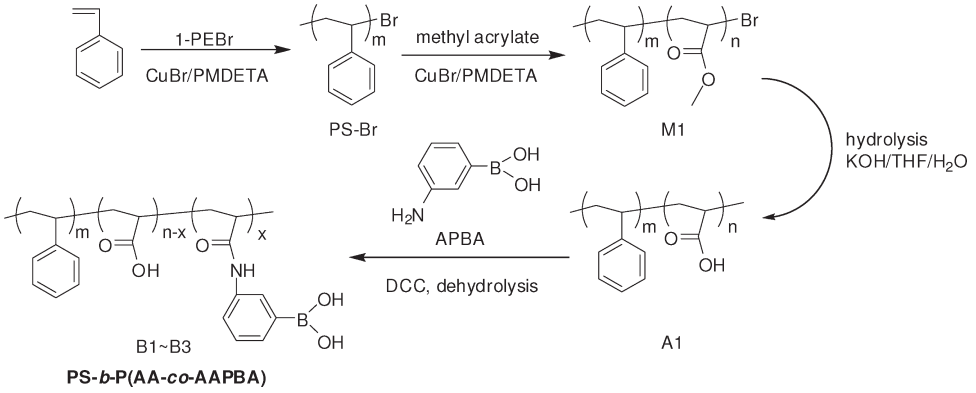

dopamine, and other biologically relevant entities.[35−42] Binding of a boronic acid to the catechol diol of Alizarin Red S (ARS) would remove the active protons, which are responsible for a large fluorescence quenching of ARS.[43,44] In other words, the formation of ARS−PBA complex can greatly increase the fluorescence intensity of ARS. Using ARS as the probe of segregated PBA groups can avoid fluorescence background caused by fluorescein adsorption and hence provide a fairly reliable and direct method to elucidate the surface segregation of hydrophilic groups or blocks. In the present work, we synthesized a novel block copolymer containing PBA pendants and fabricated them into HPPFs via the BF method. The segregation of PBA pendants in the films was investigated with ARS as the fluorescent probe. Moreover, the functional porous films with segregated PBA pendants were applied to glucose sensing.

EXPERIMENTAL SECTION

Materials. Styrene (St) and methyl acrylate (MA) were commercially obtained from Sinopharm Chemical Reagent Co. Ltd. and distilled under reduced pressure before use. CuBr was purified by successively washing with acetic acid and methanol and drying under reduced pressure. 3-Aminophenylboronic acid was recrystallized from ethanol/water (vol/vol, 40/60) mixture. Alizarin Red S (ARS) was used as received from Aldrich. Poly(ethylene terephthalate) (PET) film was kindly provided by Hangzhou Tape Factory and cleaned with acetone for 2 h before use. Water employed in all experiments was deionized and ultrafiltrated to 18.2 MΩ with an ELGA LabWater system. All other reagents were analytical grade and used without further purification.

Synthesis of PS-*b*-PAA. Polystyrene-*block*-poly(acrylic acid), PS_{141}-*b*-PAA_{14} (M_n = 17 700, M_w/M_n = 1.33), was synthesized by ATRP according to a reported procedure.[45] Briefly, St, 1-PEBr, CuBr, and PMDETA were added into a round-bottomed flask with magnetic stirring bar. The flask was degassed by three freeze−pump−thaw cycles, sealed in nitrogen, and immersed into oil bath at 110 °C while being stirred. After a prescribed time, the flask was exposed to air and the solution was diluted with tetrahydrofuran (THF). The polymer was precipitated in methanol followed by infiltration and dried under reduced pressure at 40 °C. Chain extension was performed in a similar manner. MA mixed with PS macroinitiator, CuBr, PMDETA, and *N*,*N*′-dimethylformamide (DMF) were added into a round-bottomed flask with magnetic stirring bar. After three freeze−pump−thaw cycles, the flask was sealed and immersed into oil bath at 80 °C while being stirring. After a prescribed time, the copolymer polystyrene-*block*-poly(methyl acrylate), PS-*b*-PMA, was precipitated in methanol and dried under reduced pressure at 40 °C. ^{1}H NMR (500 MHz, $CDCl_3$, δ_H, ppm): 6.23−7.30 (br, aromatic proton), 3.66 (s, −COO−CH_3), 0.79−2.48 (br, proton of backbone).

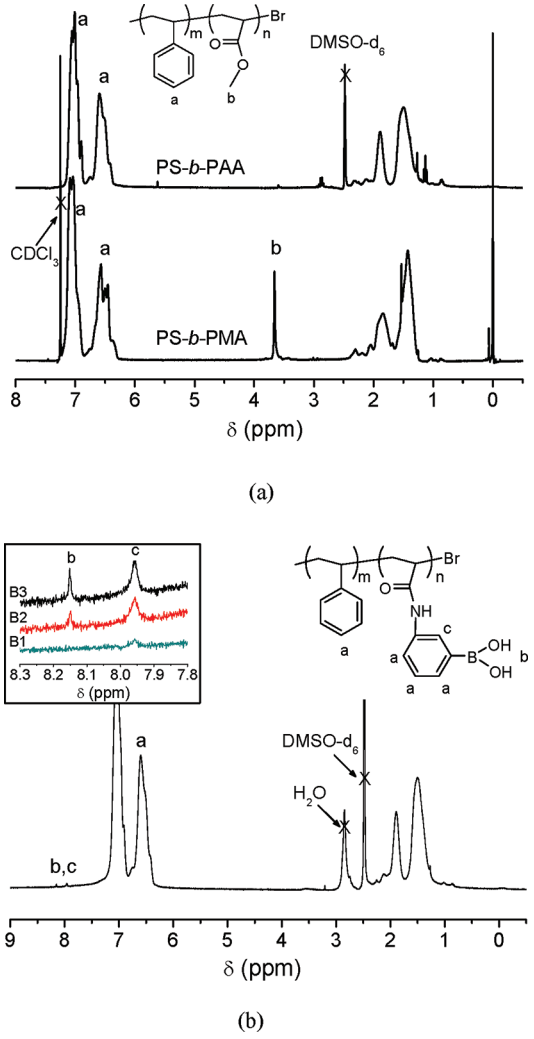

Figure 1. ^{1}H NMR spectra of (a) PS-*b*-PMA (in $CDCl_3$) and PS-*b*-PAA (in DMSO-d_6) and (b) PS-*b*-P(AA-*co*-AAPBA) with different phenylboronic acid contents (in DMSO-d_6).

The resultant PS-*b*-PMA (2.5 g) was dissolved in THF (30 mL) and hydrolyzed by adding KOH aqueous solution (40 wt %, 10 mL) and

dx.doi.org/10.1021/la201911f |*Langmuir* 2011, 27, 12597−12605

Table 1. Results of the Synthesis of PS-*b*-P(AA-*co*-AAPBA)

no.	sample	[AA]:[APBA][a]	% boron[b]	$M_{n,GPC}$	$M_{n,cal}$	MWD
M1	PS_{141}-*b*-PMA_{14}	—	—	17 300	15 900[c]	1.29
A1	PS_{141}-*b*-PAA_{14}	—	—	17 700	15 700[c]	1.33
B1	PS_{141}-*b*-P($AA_{5.4}$-*co*-$AAPBA_{8.6}$)	2:1	0.557	17 300	16 700[d]	1.31
B2	PS_{141}-*b*-P($AA_{2.6}$-*co*-$AAPBA_{11.4}$)	1:1	0.715	17 000	17 000[d]	1.31
B3	PS_{141}-*b*-P($AA_{0.5}$-*co*-$AAPBA_{13.5}$)	1:2	0.883	18 100	17 300[d]	1.33

[a] The molar ratio of carboxyl groups in the copolymers (AA) to 3-aminophenylboronic acid (APBA) in feed. [b] Calculated from the results of elemental analysis. [c] Estimated according to the ^{1}H NMR spectra. [d] Estimated according to the content of boron.

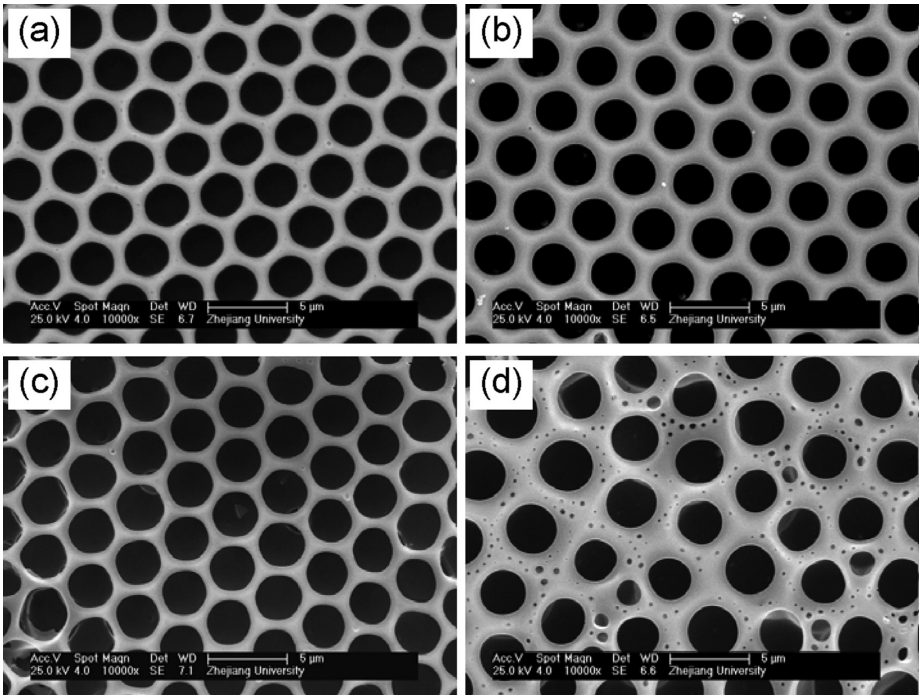

Figure 2. FESEM images of honeycomb-patterned porous films prepared from (a) **A1**, (b) **B1**, (c) **B2**, and (d) **B3** at 86%−88% RH.

triethylamine (3 mL) under reflux for 48 h. The product, polystyrene-*block*-poly(potassium acrylate), PS-*b*-PKAA, was precipitated in methanol and dried under reduced pressure. Afterward, PS-*b*-PKAA (1.5 g) was dissolved in THF (18 mL) and acidified by hydrochloric acid (1 mL) at ambient temperature for 20 h. The product was purified by petroleum ether and dried under reduced pressure at 40 °C to give PS-*b*-PAA. ^{1}H NMR (500 MHz, DMSO-d_6, δ_H, ppm): 6.25−7.35 (br, aromatic proton), 0.50−2.41 (br, proton of backbone).

Synthesis of PS-*b*-P(AA-*co*-AAPBA) Containing PBA Pendants. PS_{141}-*b*-PAA_{14} (0.4 g), THF (16 mL), *N*,*N*′-dicyclohexylcarbodiimide (DCC, 0.2 g), and a certain amount of 3-aminophenylboronic acid (APBA) were added into a round-bottomed flask with magnetic stirring bar. After 24 h of stirring at ambient temperature, the reaction mixture turned turbid and a white solid was centrifugated off. Subsequently, the supernatant was concentrated by rotary evaporation and then dropwise poured into methanol. The resulting product polystyrene-*block*-poly(acrylic acid-*co*-acrylamidophenylboronic acid) (designated as PS-*b*-P(AA-*co*-AAPBA)) was filtered, washed with methanol several times, and dried to constant weight under reduced pressure at 40 °C. ^{1}H NMR (500 MHz, DMSO-d_6, δ_H, ppm): 8.15 (s, −B(O*H*)$_2$), 7.95 (s, the aromatic proton between amide and boronic acid), 6.25−7.51 (br, aromatic proton), 0.75−2.33 (br, proton of backbone). Elemental anal.: **B1**, N 0.721, C 86.6, H 7.47; **B2**, N 0.926, C 86.4, H 7.50; **B3**, N 1.14, C 86.4, H 7.49.

Fabrication of Honeycomb-Patterned Porous Films. PS-*b*-P(AA-*co*-AAPBA) was dissolved in carbon disulfide to form a homogeneous solution with a concentration of 10 mg/mL. An aliquot of 100 μL for each polymer solution was drop-cast onto a PET film placed under a humid airflow (25 °C and >80% RH). The humid airflow was produced by bubbling a nitrogen flow through deionized water. The nitrogen flow rate is 1 L/min. Larger flow rate may lead to higher relative humidity. The effective area of the flow is about 8.6 cm^2. Owing to the condensation of water vapor on the solution surface during the evaporation of carbon disulfide, the transparent solution soon turned turbid. After solidification, the film was dried at room temperature.

Immobilization of Alizarin Red S on the Honeycomb-Patterned Porous Films. A piece of HPPF (2 × 2 cm^2) was first prewetted by immersing it into ethanol. After being completely wetted, the white HPPF turned semitransparent, indicating ethanol has infiltrated into the pores. Subsequently, the film was washed with Tris-HCl buffer solution (pH 7.40, 50 mM Tris, 44.7 mM HCl) to exchange the ethanol. After being fully wetted with Tris-HCl buffer, the film was immersed into 0.8 mL of ARS solution with a concentration of 0.1 mg/mL in Tris-HCl buffer and incubated at 25 °C for 3 h. Then the film was washed with Tris-HCl buffer solution three times. After being dried under reduced pressure at room temperature, the ARS-immobilized films were observed by confocal laser scanning microscopy (CLSM).

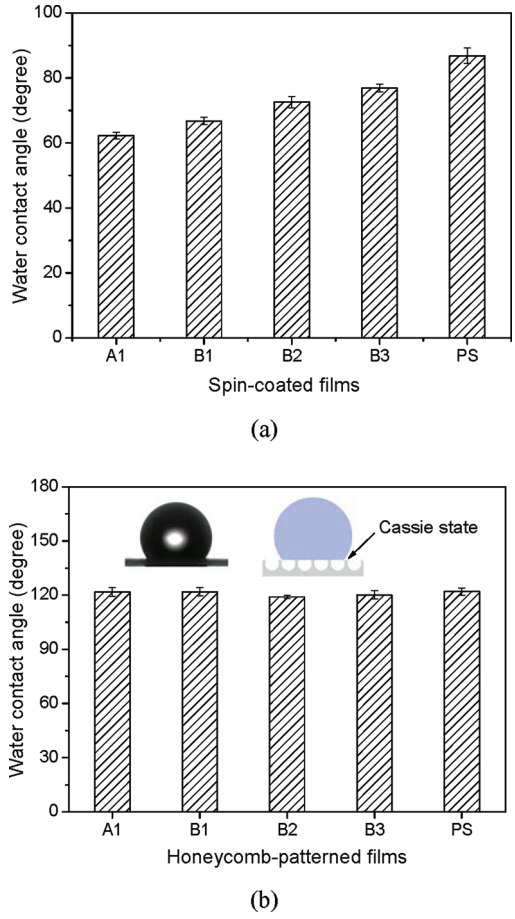

Figure 3. Water contact angles of (a) spin-coated dense films and (b) honeycomb-patterned films prepared from **A1**, **B1**, **B2**, **B3**, and PS_{141}—Br.

CLSM was carried out on a TCS SP5 confocal microscope (Leica) by exciting at λ = 455 nm and using a 550—620 nm filter for the emission.

Glucose Sensing with the Honeycomb-Patterned Porous Films. HPPFs were fabricated on the gold-coated electrode (5 MHz, AT-cut quartz crystal, Maxtek) of a quartz crystal microbalance (QCM, Resonant Probes GmbH, Goslar) by the BF method. Dense films were fabricated by spin-coating (3000 rpm for 40 s) polymer solution with a concentration of 15 mg/mL in carbon disulfide onto the gold-coated electrode. Then the resultant films were dried under reduced pressure at ambient temperature. The QCM was first primed with Tris-HCl buffer solution for 15 min at room temperature, rinsed with water, and then dried under flowing nitrogen until stable baselines were established. Thereafter, similar procedures were repeated but changing the Tris-HCl buffer solution to glucose solution with a certain concentration. A reduction in oscillation frequency of QCM was monitored after the absorption of glucose on the films.

Characterizations. Proton nuclear magnetic resonance (^{1}H NMR) spectra were recorded on a Bruker (Advance DMX500) NMR instrument with tetramethylsilane (TMS) as the internal standard, using $CDCl_3$ as the solvent at room temperature or DMSO-d_6 as the solvent at 120 °C. Fourier transform infrared (FTIR) spectra were collected on a Nicolet FTIR/Nexus 470 spectrometer. Thirty-two scans were taken for each spectrum at a nominal resolution of 1 cm^{-1}. Molecular weight and molecular weight distribution were measured by a PL 220 GPC instrument at 25 °C, which was equipped with a Waters 510 HPLC pump, three Waters Ultrastyragel columns (500, 103, and 105 Å), and a Waters 410 DRI detector. THF was used as the eluent at a flow rate of 1.0 mL/min. The calibration of the molecular weights was based on polystyrene standards. Elemental analysis was completed on a Flash EA-1112 analyzer (Carlo Erba). The relative humidity and temperature of the air flow were measured using an exact hygro-thermograph (DT-321S, CEM Corp.). A field emission scanning electron microscope (FESEM, Sirion-100, FEI) was used to observe the surface morphology of the films after being sputtered with gold (JFC-1100). Fluorescence spectra were recorded with a fluorescence spectrophotometer (RF-3510PC, Shimadzu). Water contact angles of films were measured by the sessile drop method using a DropMeter A-200 contact angle system (MAIST Vision Inspection & Measurement Ltd. Co.) at room temperature. First, a 2 μL drop of water was set onto the dry film with a microsyringe. Digital images for the droplet were then recorded. Contact angles were calculated from these images with software. Each reported value is an average of at least eight independent measurements.

RESULTS AND DISCUSSION

Synthesis of PS-*b*-P(AA-*co*-AAPBA) Containing PBA Pendants. Boronic acid-containing polymers possess unique stimuli responsivity because the formation of boronate can be effectively modulated by pH, temperature, and diol compounds.[34,35] These polymers have been usually prepared by free radical polymerization, which significantly limits the application in fields requiring polymers with well-defined structures. Most recently, Cambre and Cui et al. synthesized boronic acid-containing amphiphilic block copolymers via reversible addition—fragmentation chain transfer (RAFT) polymerization or ATRP using organic boron or silicone monomers.[46,47] In this work, a PBA-containing block copolymer, polystyrene-*block*-poly(acrylic acid-*co*-acrylamidophenylboronic acid) [PS-*b*-P(AA-*co*-AAPBA)], was synthesized from common monomers by the combination of ATRP and subsequent chemical coupling. The synthesis route is shown in Scheme 1. In the first step, macroinitiator PS was prepared via a typical ATRP process using 1-PEBr as the initiator, CuBr as the catalyst, and PMDETA as the ligand. Afterward, the hydrophilic block that has reactive carboxyl groups was introduced through chain extension with methacrylate monomer, hydrolysis of the ester group, and subsequent acidification. Figure 1a shows the ^{1}H NMR spectra of PS-*b*-PMA and PS-*b*-PAA. The peak at 3.66 ppm that belongs to the methyl proton of the ester group disappears, which demonstrates that PS-*b*-PMA has been fully converted into PS-*b*-PAA. The FT-IR spectra indicate that the strong peak at 1737 cm^{-1} induced by the carbonyl group in PS-*b*-PMA shifts to 1567 cm^{-1} after hydrolysis to PS-*b*-PKAA and eventually turns back to 1737 cm^{-1} for PS-*b*-PAA (Figure S1, Supporting Information). GPC analysis shows that the number-average molecular weight (M_n) and molecular weight distribution (MWD) of PS-*b*-PAA are 17 700 g/mol and 1.33, respectively (Table 1).

PBA was introduced as pendant group through the reaction of amine-terminated PBA (APBA) with the carboxyl groups of PS-*b*-PAA using DCC as the coupling agent. Copolymers with different PBA contents were synthesized by changing the APBA:AA ratios in the feed (Table 1). Figure 1b displays the ^{1}H NMR spectra of PS-*b*-P(AA-*co*-AAPBA). It can be seen that the characteristic peaks of PBA at 7.9—8.2 ppm appear. The FT-IR spectra (Figure S2, Supporting Information) show that the strong peak at 1737 cm^{-1} decreases and the characteristic peak at 1344 cm^{-1} for B—O bond strengthens. Moreover, the bands at 1662 and 1546 cm^{-1}, which are assigned to amide groups, clearly emerge in the spectra of PS-*b*-P(AA-*co*-AAPBA).

Scheme 2. Schematic Illustration of the Interaction among Alizarin Red S (ARS), Saccharide, and Phenylboronic Acid (PBA)

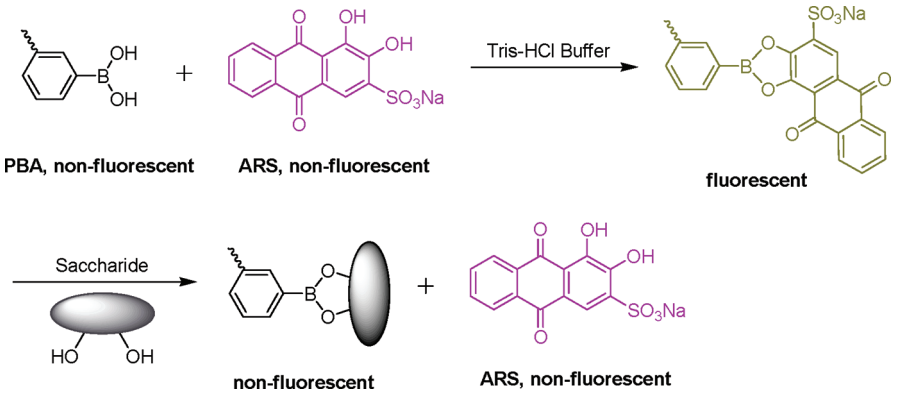

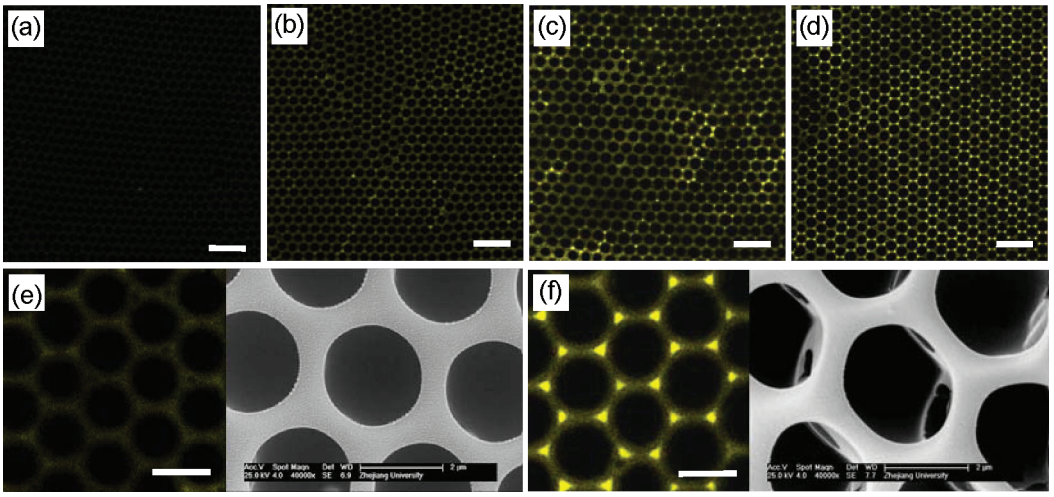

Figure 4. Fluorescence images of honeycomb-patterned porous films after adsorption of ARS: (a) **A1**, (b) **B1**, (c) **B2**, (d) **B3**, and (e, f) the corresponding images of parts b and d. Scale bar: a−d, 10 μm; e and f, 3 μm.

These characteristic peaks provide a solid evidence for the covalent binding of PBA as pendant groups. The contents of PBA in the block copolymers were measured by elemental analysis.[48] As shown in Table 1, for **B1**, **B2**, and **B3** the APBA: AA molar ratios in feed are 1:2, 1:1, 2:1, respectively, and the resultant content of boron increases from 0.557% to 0.883%. GPC analysis illustrates that the M_n increases slightly with PBA content and the MWD remains narrow (1.31−1.33).

Regularity and Pore Size of Honeycomb-Patterned Porous Films. HPPFs were prepared from the PBA-containing copolymers via a typical BF procedure. A solvent mixture of CS_2 and CH_2Cl_2 in the ratio of 85:15 (v/v) was utilized to dissolve the copolymers, especially those with high PBA content. Each polymer was cast at least 20 times with ranging conditions to obtain reproducible and reliable results.

It has been elucidated that the pore size and regularity are profoundly influenced by a range of casting conditions, such as humidity and polymer concentration. In our cases, the relative humidity and the composition of copolymers are two key factors for the preparation of highly ordered macroporous films. Our previous study has ascertained that PS is able but unlikely to form an ordered honeycomb structure.[13] After introducing the hydrophilic block, both the regularity and the repeatability of the films are significantly improved (Figure 2a). This could be attributed to the surface-activity of the amphiphilic copolymer, i.e., encapsulating the water droplets, preventing the water droplets from coalescing, and thus stabilizing the arrays of water droplets.[8,10] Comparing with PAA block, the PBA pedant is more hydrophobic, as confirmed by the water contact angles of the corresponding spin-coated films (Figure 3a). PS_{141}-*b*-P($AA_{0.5}$-*co*-$AAPBA_{13.5}$) that has the highest content of PBA pedant results in films with the lowest regularity (Figure 2). However, the pore diameter changes little, ranging from 2.34 to 2.80 μm.

Since the water droplet array acts as a sacrificed template for the pore formation during the BF process, the relative humidity of airflow determines the availability of moisture to form ordered pore structure. Experimentally, ordered pore arrays cannot be obtained at humidity below 83% (Figure S3, Supporting Information). After increasing the humidity to 86−88%, highly ordered and uniform pores are formed. When the humidity is between 91% and 93%, the film regularity decreases obviously. Copolymers **B1** and **B2** are more hydrophilic than **B3**; hence, highly regular films can be achieved at a low humidity (86−88%). As for the most hydrophobic copolymer **B3**, high humidity (91−93%) is preferable. Meanwhile, higher humidity leads to larger pores. For example, the average pore diameter of **B3** film

Scheme 3. Schematic Illustration of the Interconnected Pore Structure and the Distribution of Phenylboronic Acid Pendants in the Honeycomb-Patterned Films

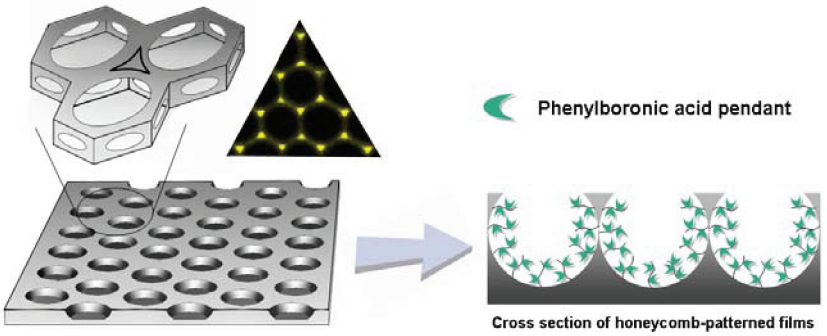

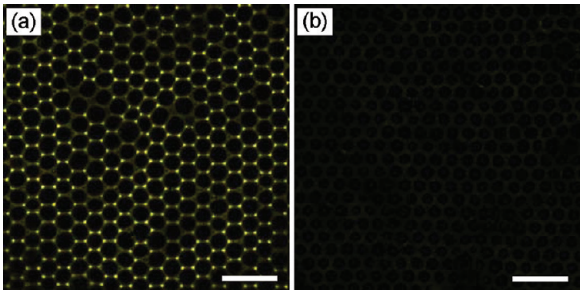

Figure 5. Fluorescence images of ARS-immobilized **B3** honeycomb-patterned porous films (a) after being prewetted with ethanol and (b) without being prewetted. Scale bar: 10 μm.

increases from 0.83 to 3.25 μm with relative humidity increasing from 80% to 93%. These results can be explained as follows. At low humidity the moisture is not sufficient to form homogeneous water droplet arrays, and the corresponding size of droplets is small. On the other hand, high humidity rapidly results in water droplets with large size and it is difficult to avoid the coalescence, which eventually leads to a disordered pore structure.[8,10,49]

Distribution of Phenylboronic Acid Groups in the Honeycomb-Patterned Porous Films. During the BF process, it is believed that hydrophilic blocks tend to aggregate themselves around the water droplets because of the mutual interaction. After the evaporation of water, porous films with polar functional groups enriched inside the pores and hydrophobic blocks enriched on the external surface were achieved.[22,25,50,51] In our case, the enrichment of hydrophilic P(AA-*co*-AAPBA) block is expected. To investigate the distribution of PBA groups, a fluorescent probe ARS was used to detect PBA. ARS does not emit fluorescence itself but can intensely emit fluorescence after reacting with PBA (Scheme 2).[43] Nevertheless, we found that ARS remained quenched in the APBA/ARS mixture (Figure S4, Supporting Information), which might be due to effects of the lone-pair electrons from the amino groups. Interestingly, a high intensity of fluorescence was observed for the ARS/acrylamidophenylboronic acid (AAPBA) mixture. As AAPBA has a similar structure with the PBA pendants in the copolymers, this specific fluorescence feature of ARS not only avoids undesirable fluorescent background, but also provides a powerful technique to evidence the chemical binding between PS-*b*-PAA and APBA.

Figure 3b shows water contact angles on the HPPFs. According to the Cassie and Baxter law, the contact angles (θ_M) can be theoretically calculated as

$$\cos\theta_M = (1 - f_{pore})\cos\theta_{polymer} - f_{pore} \quad (1)$$

where f_{pore} is the area fraction of pores and $\theta_{polymer}$ is the water contact angle of a polymer in the form of a thin and smooth film. The f_{pore} estimated from the SEM images is about 0.52. We assume that the outer surface layer of the honeycomb film is mainly composed of polystyrene. Considering that θ_{PS} is 89°, the calculated θ_M of the honeycomb-patterned films is about 122°, which is very close to the experimental results (~120°). That means that the highly porous film cannot be wetted by water, forming a Cassie state.[32,52] Therefore, the PS-*b*-P(AA-*co*-AAPBA) film has a hydrophobic surface and needs to be prewetted with ethanol to induce a Cassie–Wenzel transition before immersion into ARS solution, thus allowing the penetration of ARS solution into the pores. Fluorescence images show that the fluorescence intensity of the ARS-immobilized films increases with the content of PBA (Figure 4 and Supporting Information, Figure S5). Particularly, an ordered array of triangular fluorescent spots can be observed for **B3** sample [PS_{141}-*b*-P($AA_{0.5}$-*co*-$AAPBA_{13.5}$), Figure 4d]. This is due to the special pore morphology of **B3** film, as revealed by the SEM image (Figure 4f). Copolymer **B3** that has the highest content of PBA is no longer hydrophilic enough to perfectly encapsulate water droplets. Hence an interconnected pore structure is obtained. As a result, the density of PBA pendants at the intersection of three adjacent pores is larger than surroundings, and hence, the intersection area exhibits a triangular spot with strong fluorescence (Scheme 3). These special triangular spots compose the fluorescence arrays, which make the sensing visible. For copolymers with low content of PBA (e.g., **B1** and **B2**), the pores of the HPPFs are not interconnected (Figure 4e). Confocal depth profiling can also be made along the *z*-axis to generate a series of CLSM images (Figure S6, Supporting Information), which confirm that the PBA pendants are mainly distributed on the pore surface.

To further verify the distribution of PBA, porous films that were directly immersed into ARS solution without being prewetted were also characterized by CLSM (Figure 5). The fluorescence intensity of the film is very weak. That means the PBA pendants, which react with ARS and then emit fluorescence, are mainly distributed at the pore wall, instead of at the outer surface layer of the films.

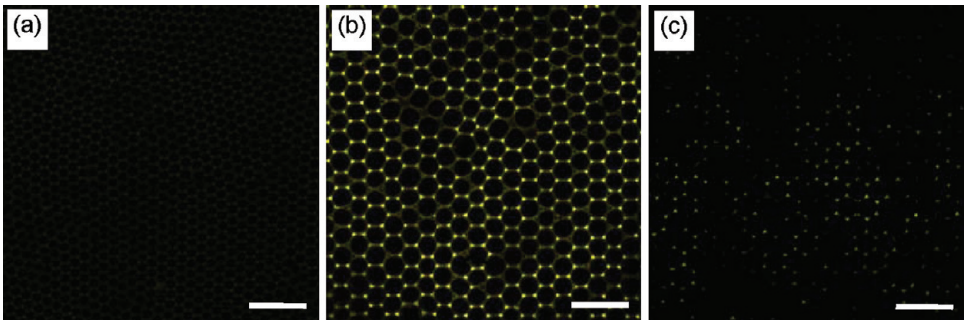

Figure 6. Fluorescence images of (a) **A1**, (b) ARS-immobilized **B3** honeycomb-patterned porous films, and (c) sample in part b being exposed to 1 M of glucose solution. Scale bar: 10 μm.

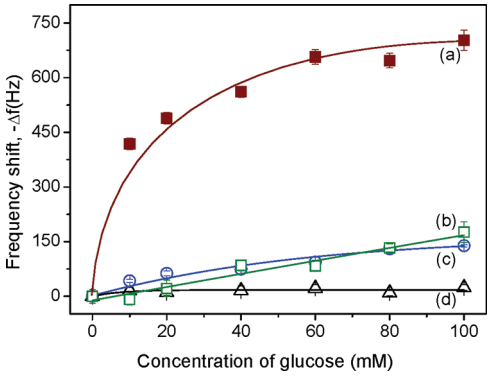

Figure 7. QCM results of different films exposed to glucose solution. **B3** honeycomb-patterned porous films (a) after being prewetted with ethanol and (b) without being prewetted, (c) **B3** dense films, and (d) **A1** honeycomb-patterned porous films after being prewetted with ethanol.

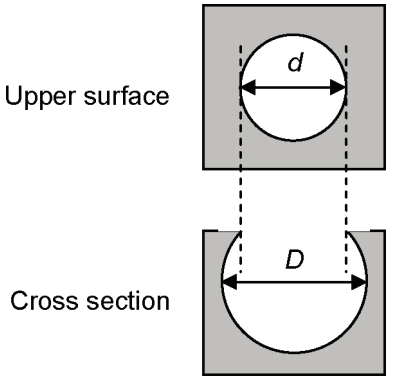

Figure 8. Illustration of the estimation of the specific surface area of honeycomb-patterned films.

Glucose Sensing with the Honeycomb-Patterned Porous Films. As mentioned above, PBA groups are mainly distributed at the pore surface of the HPPFs during the BF process. Therefore, it is speculated that the PBA-functionalized films have potential in sensing glucose. Qualitatively, fluorescence spectroscopy was used to confirm the interaction between glucose and the PBA-functionalized films. It is reported that the association constant between Alizarin and phenylboronic acid is 282 times higher than that between glucose and phenylboronic acid at pH 7.4.[34] Therefore, an excess of glucose (1 M) was used to replace the immobilized Alizarin. As shown in Figure 6 and Supporting Information Figure S5, it is clear that glucose can effectively quench the fluorescence of ARS-immobilized film. It is because glucose can replace the ARS and complex with the PBA groups. The released free ARS is not able to emit fluorescence.

Quantitatively, sensing of glucose was investigated based on QCM at physiological pH. Generally, the concentration of sugar (mainly glucose) in persons with diabetes is higher than 10 mM. Therefore, the QCM experiments were performed with glucose concentration ranging from 10 to 100 mM. As shown in Figure 7, curve a demonstrates the effective binding of PBA-functionalized HPPF with glucose because the oscillation frequency shifts obviously whereas low shifts can be observed in the controlled experiment (curve d). Curve c corresponds to a PS-*b*-P(AA-*co*-AAPBA) dense film. Since most of PBA pendants were buried inside the bulk of the dense film and only the outer surface of film could contact with the solution, the resultant frequency shift was very low. Curve b is the result of PS-*b*-P(AA-*co*-AAPBA) HPPF without being prewetted. The low frequency shifts indicates that only small amounts of PBA pendants locate at the external surface.

To further confirm the reason for high glucose responsivity of PBA-functionalized HPPFs, the ratio of the surface area (S_1) of a typical HPPF to that of a smooth dense film (S_2) was estimated (Figure 8). We assume the pore is a part of a sphere. The diameters of d and D can be obtained from the surface and cross section SEM images, and the pore fraction (f) can also be obtained from the surface SEM images. Therefore, S_1/S_2 can be estimated according to the following equations:

$$S_1/S_2 = \frac{f}{\pi(d/2)^2} A_{\text{pore}} + (1-f) \quad (2)$$

$$A_{\text{pore}} = \left[1 - \frac{\arcsin(d/D)}{\pi}\right] \pi D^2 \quad (3)$$

In our case, d = 2.70 μm, D = 3.30 μm, and f = 0.52. Therefore, S_1/S_2 is about 2.6. Obviously, HPPFs own larger surface area compared with spin-coated films. On the other hand, based on the QCM results, the response ratio of the HPPF to the corresponding dense film (R_1/R_2) at 60 mM of glucose is about 7.1, which is obviously larger than S_1/S_2. Therefore, we conclude that not only the large specific surface area of the HPPF but also the segregation of PBA pendants account for the sensitive glucose sensing.

It should be mentioned that the thickness of the films may have an influence on the sensing results. In this work, the films were prepared from a fixed volume of polymer solution to control the thickness, which can be measured from the cross section SEM images (Figure S7, Supporting Information). The apparent

thickness of the film is about 3 μm. This is a large thickness that may exceed the detection limit of QCM and make the sensing infeasible. But, as we know, the film is highly porous and the effective thickness is far less than 3 μm. Therefore, the frequency shift, Δf, for the PBA-functionalized HPPFs is up to about 700 Hz, which is comparable to those reported in the literature.[53] On the other hand, we have demonstrated that both the surface segregation of PBA groups and the porous structures are key factors affecting the sensing results. The film thickness displays relatively slight influence. A thickness that is in the detection limit of QCM is acceptable in our cases.

CONCLUSIONS

In summary, we proposed a facile approach to the fabrication of phenylboronic acid (PBA) arrays for glucose sensing. An amphiphilic copolymer containing PBA pendants has been synthesized by ATRP and subsequent chemical coupling. Honeycomb-patterned porous films (HPPFs) were prepared by casting the copolymer solution under humid airflows. We found that the regularity and pore size of the films were mainly determined by the composition of the copolymers and the relative humidity of airflow. The segregation of PBA pendants at the pore wall was clearly demonstrated through controlling the surface wetting by the ARS aqueous solution. Using nonfluorescent ARS as the probe can completely avoid fluorescence background induced by fluorescein adsorption. This investigation contributes a convincing way to determine the distribution of hydrophilic groups in the breath figures. Furthermore, the porous structure endows the films large specific surface area. Both this feature and the surface segregation of PBA pendants account for the sensitive glucose sensing by the PBA-functionalized HPPFs.

ASSOCIATED CONTENT

Supporting Information. FTIR characterization of the copolymer; fluorescence spectra of ARS−AAPBA complex; FESEM images of HPPFs fabricated from **B1**, **B2**, and **B3** under different relative humidity; step scanning CLSM images of ARS-immobilized **B3** HPPF; and fluorescence intensity of ARS-immobilized films. This material is available free of charge via the Internet at http://pubs.acs.org.

AUTHOR INFORMATION

Corresponding Author

*E-mail: lswan@zju.edu.cn. Tel: +86-57187953763. Fax: +86-57187951592.

ACKNOWLEDGMENT

Financial support from the National Natural Science Foundation of China (51173161, 50803053), the Zhejiang Provincial Natural Science Foundation of China (Y4110076), the Program for Zhejiang Provincial Innovative Research Team (2009R50004), and the Open Fund of Zhejiang Provincial Top Key Discipline of New Materials and Process Engineering (20110932) is gratefully acknowledged. We thank Dr. Bin-Yang Du of Zhejiang University for the use of the QCM.

REFERENCES

(1) Campbell, M.; Sharp, D. N.; Harrison, M. T.; Denning, R. G.; Turberfield, A. J. *Nature* **2000**, *404*, 53–56.
(2) Hu, X. B.; Li, G. T.; Li, M. H.; Huang, J.; Li, Y.; Gao, Y. B.; Zhang, Y. H. *Adv. Funct. Mater.* **2008**, *18*, 575–583.
(3) Gates, B.; Yin, Y. D.; Xia, Y. N. *Chem. Mater.* **1999**, *11*, 2827–2836.
(4) Corma, A.; Davis, M. E. *ChemPhysChem* **2004**, *5*, 304–313.
(5) Erdogan, B.; Song, L. L.; Wilson, J. N.; Park, J. O.; Srinivasarao, M.; Bunz, U. H. F. *J. Am. Chem. Soc.* **2004**, *126*, 3678–3679.
(6) Schmid, H.; Michel, B. *Macromolecules* **2000**, *33*, 3042–3049.
(7) Widawski, G.; Rawiso, M.; Francois, B. *Nature* **1994**, *369*, 387–389.
(8) Bunz, U. H. F. *Adv. Mater.* **2006**, *18*, 973–989.
(9) Srinivasarao, M.; Collings, D.; Philips, A.; Patel, S. *Science* **2001**, *292*, 79–83.
(10) Stenzel, M. H.; Barner-Kowollik, C.; Davis, T. P. *J. Polym. Sci., Part A: Polym. Chem.* **2006**, *44*, 2363–2375.
(11) Connal, L. A.; Vestberg, R.; Hawker, C. J.; Qiao, G. G. *Adv. Funct. Mater.* **2008**, *18*, 3706–3714.
(12) Liu, C. H.; Gao, C.; Yan, D. Y. *Angew. Chem., Int. Ed.* **2007**, *46*, 4128–4131.
(13) Ke, B. B.; Wan, L. S.; Zhang, W. X.; Xu, Z. K. *Polymer* **2010**, *51*, 2168–2176.
(14) Li, L.; Zhong, Y. W.; Ma, C. Y.; Li, J.; Chen, C. K.; Zhang, A. J.; Tang, D. L.; Xie, S. Y.; Ma, Z. *Chem. Mater.* **2009**, *21*, 4977–4983.
(15) Hirai, Y.; Yabu, H.; Matsuo, Y.; Ijiro, K.; Shimomura, M. *Chem. Commun.* **2010**, *46*, 2298–2300.
(16) Fukuhira, Y.; Kitazono, E.; Hayashi, T.; Kaneko, H.; Tanaka, M.; Shimomura, M.; Sumi, Y. *Biomaterials* **2006**, *27*, 1797–1802.
(17) Tang, P. Q.; Hao, J. C. *Langmuir* **2010**, *26*, 3843–3847.
(18) Park, J. S.; Lee, S. H.; Han, T. H.; Kim, S. O. *Adv. Funct. Mater.* **2007**, *17*, 2315–2320.
(19) Zhao, B. H.; Zhang, J.; Wang, X. D.; Li, C. X. *J. Mater. Chem.* **2006**, *16*, 509–513.
(20) Nomura, E.; Hosoda, A.; Takagaki, M.; Mori, H.; Miyake, Y.; Shibakami, M.; Taniguchi, H. *Langmuir* **2010**, *26*, 10266–10270.
(21) Wan, L. S.; Jie, L.; Ke, B. B.; Xu, Z. K. *ACS Appl. Mater. Interfaces* **2010**, *2*, 3759–3765.
(22) Galeotti, F.; Calabrese, V.; Cavazzini, M.; Quici, S.; Poleunis, C.; Yunus, S.; Bolognesi, A. *Chem. Mater.* **2010**, *22*, 2764–2769.
(23) Zhang, Y.; Wang, C. *Adv. Mater.* **2007**, *19*, 913–916.
(24) Munoz-Bonilla, A.; Ibarboure, E.; Bordege, V.; Fernandez-Garcia, M.; Rodriguez-Hernandez, J. *Langmuir* **2010**, *26*, 8552–8558.
(25) Ke, B. B.; Wan, L. S.; Xu, Z. K. *Langmuir* **2010**, *26*, 8946–8952.
(26) Wang, C. Y.; Mao, Y. D.; Wang, D. Y.; Qu, Q. S.; Yang, G. J.; Hu, X. Y. *J. Mater. Chem.* **2008**, *18*, 683–690.
(27) Cui, L.; Xuan, Y.; Li, X.; Ding, Y.; Li, B. Y.; Han, Y. C. *Langmuir* **2005**, *21*, 11696–11703.
(28) Wan, L. S.; Ke, B. B.; Li, X. K.; Meng, X. L.; Zhang, L. Y.; Xu, Z. K. *Sci. China Ser. B-Chem.* **2009**, *52*, 969–974.
(29) Boker, A.; Lin, Y.; Chiapperini, K.; Horowitz, R.; Thompson, M.; Carreon, V.; Xu, T.; Abetz, C.; Skaff, H.; Dinsmore, A. D.; Emrick, T.; Russell, T. P. *Nat. Mater.* **2004**, *3*, 302–306.
(30) Sun, W.; Ji, J.; Shen, J. C. *Langmuir* **2008**, *24*, 11338–11341.
(31) Jiang, X. L.; Zhou, X. F.; Zhang, Y.; Zhang, T. Z.; Guo, Z. R.; Gu, N. *Langmuir* **2010**, *26*, 2477–2483.
(32) Ke, B. B.; Wan, L. S.; Chen, P. C.; Zhang, L. Y.; Xu, Z. K. *Langmuir* **2010**, *26*, 15982–15988.
(33) Escale, P.; Save, M.; Lapp, A.; Rubatat, L.; Billon, L. *Soft Matter* **2010**, *6*, 3202.
(34) Springsteen, G.; Wang, B. H. *Tetrahedron* **2002**, *58*, 5291–5300.
(35) Wang, B. L.; Ma, R. J.; Liu, G.; Li, Y.; Liu, X. J.; An, Y. L.; Shi, L. Q. *Langmuir* **2009**, *25*, 12522–12528.
(36) Liu, Y.; Deng, C.; Tang, L.; Qin, A.; Hu, R.; Sun, J. Z.; Tang, B. Z. *J. Am. Chem. Soc.* **2011**, *133*, 660–663.
(37) Matsumoto, A.; Yoshida, R.; Kataoka, K. *Biomacromolecules* **2004**, *5*, 1038–1045.
(38) Chen, T.; Chang, D. P.; Liu, T.; Desikan, R.; Datar, R.; Thundat, T.; Berger, R.; Zauscher, S. *J. Mater. Chem.* **2010**, *20*, 3391–3395.

(39) Honda, M.; Kataoka, K.; Seki, T.; Takeoka, Y. *Langmuir* **2009**, *25*, 8349–8356.
(40) Lapeyre, V.; Renaudie, N.; Dechezelles, J. F.; Saadaoui, H.; Ravaine, S.; Ravaine, V. *Langmuir* **2009**, *25*, 4659–4667.
(41) De Geest, B. G.; Jonas, A. M.; Demeester, J.; De Smedt, S. C. *Langmuir* **2006**, *22*, 5070–5074.
(42) Wang, D.; Liu, T.; Yin, J.; Liu, S. Y. *Macromolecules* **2011**, *44*, 2282–2290.
(43) Springsteen, G.; Wang, B. H. *Chem. Commun.* **2001**, 1608–1609.
(44) Pasparakis, G.; Vamvakaki, M.; Krasnogor, N.; Alexander, C. *Soft Matter* **2009**, *5*, 3839–3841.
(45) Hu, D. J.; Cheng, Z. P.; Wang, G.; Zhu, X. L. *Polymer* **2004**, *45*, 6525–6532.
(46) Cambre, J. N.; Roy, D.; Gondi, S. R.; Sumerlin, B. S. *J. Am. Chem. Soc.* **2007**, *129*, 10348–10349.
(47) Cui, C. Z.; Bonder, E. M.; Qin, Y.; Jakle, F. *J. Polym. Sci., Part A: Polym. Chem.* **2010**, *48*, 2438–2445.
(48) Tan, J.; Wang, H. F.; Yan, X. P. *Anal. Chem.* **2009**, *81*, 5273–5280.
(49) Peng, J.; Han, Y. C.; Yang, Y. M.; Li, B. Y. *Polymer* **2004**, *45*, 447–452.
(50) Stenzel, M. H.; Davis, T. P. *Aust. J. Chem.* **2003**, *56*, 1035–1038.
(51) Ting, S. R. S.; Min, E. H.; Escale, P.; Save, M.; Billon, L.; Stenzel, M. H. *Macromolecules* **2009**, *42*, 9422–9434.
(52) Ke, B. B.; Wan, L. S.; Li, Y.; Xu, M. Y.; Xu, Z. K. *Phys. Chem. Chem. Phys.* **2011**, *13*, 4881–4887.
(53) Liu, G. M.; Zhang, G. Z. *J. Phys. Chem. B* **2005**, *109*, 743–747.